Hybrid Q-switched Yb-doped fiber laser

J. Y. Huang, W. Z. Zhuang, W. C. Huang, K. W. Su, K. F. Huang, and Y. F. Chen*

Department of Electrophysics, National Chiao Tung University, Hsinchu, Taiwan
* yfchen@cc.nctu.edu.tw

Abstract: We investigate the performance of a hybrid Q-switched (HQS) fiber laser that is constructed with a low RF-power driven acousto-optic (AO) Q-switch and an AlGaInAs semiconductor saturable absorber. Compared to a pure passively Q-switched (PQS) fiber laser, the ratio of timing jitter to pulse period can be significantly reduced from 2% to 0.3% in the regime of far above threshold. On the other hand, the prelasing effect in a pure actively Q-switched fiber laser can be considerably improved. More importantly, the maximum pulse energy of the HQS fiber laser can be increased approximately 25% in comparison with the result of the PQS fiber laser. At a pump power of 24 W, the highest pulse energy is up to 0.56 mJ with the pulse duration of 50 ns at the repetition rate of 23 kHz.

© 2011 Optical Society of America

OCIS codes: (140.3510) Lasers, fiber; (140.3480) Lasers, diode-pumped; (140.3540) Lasers, Q-switched.

References and links

1. J. A. Alvarez-Chavez, H. L. Offerhaus, J. Nilsson, P. W. Turner, W. A. Clarkson, and D. J. Richardson, "High-energy, high-power ytterbium-doped Q-switched fiber laser," Opt. Lett. **25**(1), 37–39 (2000).
2. Y. X. Fan, F. Y. Lu, S. L. Hu, K. C. Lu, H. J. Wang, X. Y. Dong, J. L. He, and H. T. Wang, "Tunable high-peak-power, high-energy hybrid Q-switched double-clad fiber laser," Opt. Lett. **29**(7), 724–726 (2004).
3. Z. J. Chen, A. B. Grudinin, J. Porta, and J. D. Minelly, "Enhanced Q switching in double-clad fiber lasers," Opt. Lett. **23**(6), 454–456 (1998).
4. J. Y. Huang, W. Z. Zhuang, W. C. Huang, K. W. Su, C. Hu, K. F. Huang, and Y. F. Chen, "Comparative studies for Cr^{4+}:YAG crystal and AlGaInAs semiconductor used as a saturable absorber in Q-switched Yb-doped fiber lasers," Opt. Express **17**(23), 20800–20805 (2009).
5. W. Z. Zhuang, W. C. Huang, P. Y. Chiang, K. W. Su, K. F. Huang, and Y. F. Chen, "Millijoule-level Yb-doped photonic crystal fiber laser passively Q-switched with AlGaInAs quantum wells," Opt. Express **18**(26), 27910–27915 (2010).
6. J. B. Khurgin, F. Jin, G. Solyar, C. C. Wang, and S. Trivedi, "Cost-effective low timing jitter passively Q-switched diode-pumped solid-state laser with composite pumping pulses," Appl. Opt. **41**(6), 1095–1097 (2002).
7. S. L. Huang, T. Y. Tsui, C. H. Wang, and F. J. Kao, "Timing jitter reduction of a passively Q-switched laser," Jpn. J. Appl. Phys. **38**(Part 2, No. 3A), L239–L241 (1999).
8. T. Hakulinen, R. Koskinen, and O. G. Okhotnikov, "Low jitter Q-switched fiber laser using optically driven surface-normal saturable absorber modulator," Opt. Express **16**(12), 8720–8726 (2008).
9. B. Cole, L. Goldberg, C. W. Trussell, A. Hays, B. W. Schilling, and C. McIntosh, "Reduction of timing jitter in a Q-Switched Nd:YAG laser by direct bleaching of a Cr^{4+}:YAG saturable absorber," Opt. Express **17**(3), 1766–1771 (2009).
10. D. Nodop, J. Rothhardt, S. Hädrich, J. Limpert, and A. Tünnermann, "Wavelength-independent all-optical synchronization of a Q-switched 100-ps microchip laser to a femtosecond laser reference source," Appl. Phys. B **74**, 367–374 (2002).
11. O. M. Stafsudd, O. Ersoy, and S. Pizzica, "CO_2 LASER with simultaneous active and passive Q-switching," Appl. Opt. **10**(1), 141–143 (1971).
12. X. Wang, and Z. Xu, "Single-longitudinal-mode operation of a 1 Watt combined actively and passively Q-switched Cr,Nd:YAG laser," Opt. Express **13**(18), 6693–6698 (2005).
13. M. Arvidsson, B. Hansson, M. Holmgren, and C. Lindstrom, "A combined actively and passively Q-switched microchip laser," in solid State Lasers VII, R. Scheps, ed., Proc. SPIE 3265, 106–113 (1998).
14. T. Dascalu, C. Dascalu, and N. Pavel, "Nd:YAG laser continuous wave pumped, Q-switched by hybrid 'passive-active' methods," ROMOPTO 2000: Sixth Conference on Optics, Ed. V.I. Vlad, Bucharest, Romania, September 2000, Proc. SPIE **4430**, 52–61 (2001).
15. S. C. Huang, S. C. Liu, A. Li, K. W. Su, Y. F. Chen, and K. F. Huang, "AlGaInAs quantum-well as a saturable absorber in a diode-pumped passively Q-switched solid-state laser," Opt. Lett. **32**(11), 1480–1482 (2007).

1. Introduction

Double-clad ytterbium (Yb) doped large-mode-area fiber lasers have been confirmed to possess the advantages of good heat dissipation, high efficiency, and high gain. Compared to CW fiber lasers, high-power and high-pulse-energy Q-switched fiber lasers have proved to be practically useful in various applications such as range finding, remote-sensing, and coherent lidar systems [1–3]. The Q-switched pulse energy is mainly determined by the mode field area, the lifetime of active ions, and the modulation depth of Q-switch. To achieve high-pulse-energy Yb-doped LMA Q-switched fiber lasers, a Q-switch with large modulation loss is requested. Acousto-optic modulators (AOMs) with high diffraction loss [1–3] and saturable absorbers with high modulation depth [4,5] have been recently employed as Q-switchers to obtain high-power and high-pulse-energy Yb-doped fiber lasers, respectively. The advantages of active Q-switching (AQS) are tunable repetition rate and stable pulse generation. However AOMs, or acousto-optic (AO) Q-switches demand high driving RF-power to realize high modulation losses for high power lasers. Hence the RF-power drivers and the cooling systems would be complicated. On the other hand, passive Q-switching (PQS) by saturable absorbers can operate without external driving electronics. The timing jitter, however, of PQS fiber lasers is inevitable and it would limit the availability for applications. Timing jitter is mainly attributed to the fact that lasers originate from photons of the spontaneous emission which would be affected by fluctuations of temperature in gain medium and wavelength of pump sources [6,7]. There are many works done to reduce the timing jitter for PQS lasers such as composite pump scheme [6] and optical triggering saturable absorbers by electrically controlled light sources [8–10]. The former method is limited to operate only near the lasing threshold while the latter would decrease the pulse energy owing to the pre-bleaching to saturable absorbers.

Compared to AQS and PQS, an alternative method is to use a large-modulation-depth saturable absorber and a low-RF-power driven AO Q-switch simultaneously. In the hybrid Q-switched (HQS) operation, the saturable absorber is used for generating high modulation loss while the AO Q-switch is used for reducing the timing jitter. The HQS method has been employed in CO_2 laser [11], solid-state microchip laser [12,13], and high average power solid-state laser [14]. Nevertheless, to our best knowledge hybrid Q-switched fiber lasers have not yet been investigated so far.

In this paper we investigate the performance of a HQS fiber laser that is constructed with a low RF-power driven AO Q-switch and an AlGaInAs semiconductor saturable absorber. Compared to a PQS fiber laser, the ratio of timing jitter to pulse period can be significantly reduced from 2% to 0.3% in the regime of far above threshold. On the other hand, the prelasing effect in a pure AO Q-switched fiber laser can be considerably improved. More importantly, the maximum pulse energy of the HQS fiber laser can be increased approximately 25% in comparison with the result of the PQS fiber laser. At a pump power of 24 W, the highest pulse energy is up to 0.56 mJ with the pulse duration of 50 ns at a repetition rate of 23 kHz.

2. Experimental setup

Figure 1 presents the schematic diagram of the experimental setup of the HQS Yb-doped fiber laser that consisted of a 3-m Yb-doped fiber (nLIGHT Corporation) and an external feedback cavity. The fiber has an absorption coefficient of 10.8 dB/m at 976 nm and a double-clad structure with a 350-μm octagonal outer cladding, a 250-μm inner cladding with a numerical aperture (NA) of 0.46, and a 30-μm circular core with a NA of 0.07. The fiber end facet near the external cavity was angle-cleaved to prevent Fresnel reflection and parasitic lasing and the other end facet was normal-cleaved as an output coupler with reflectivity of 4%. The external feedback cavity comprised an aspheric lens with the focal length of 25 mm, the saturable absorber, a highly reflective mirror for 1030nm~1100nm, a Fabry-Pérot thin film filter (FP filter), and an AO Q-switch. The peak of the FP filter is at 1100 nm with a full-width-at-half-maximum bandwidth of 5 nm at normal incidence. The FP filter was used here for shortening

and selecting the resonant wavelength, which was chosen as 1066 nm to match the resonant wavelength of the absorber. The AlGaInAs absorber was designed with 50 groups of three quantum wells (QWs) as described in Ref [4,15]. Both sides of the semiconductor absorber were coated for anti-reflecting to reduce back reflections and the couple-cavity effects. The saturation energy density, the initial transmission, and the final transmission of AlGaInAs QWs are 1 mJ/cm^2, 27%, and 95%, respectively [4]. The cross-section for the AlGaInAs QWs is in the order of 10^{-15} cm^2. The saturable absorber was wrapped with indium foil and mounted in a copper block without active cooling. The AO Q-switch (NEOS Technologies) is 30-mm long with AR coating at 1.06 μm on both faces and was driven at 27.12-MHz center frequency by 15-W RF power. The AO Q-switch was also mounted in a copper block. The rise time is 115 ns/mm beam diameter.

The pump source was a 30-W 976-nm fiber-coupled laser diode with a core diameter of 400 μm and a NA of 0.22. A focusing lens with 25 mm focal length and 90% coupling efficiency was used to re-image the pump beam into the fiber through a dichroic mirror with high transmission (>90%) at 976 nm and high reflectivity (>99.8%) at 1066 nm. The pump spot radius was approximately 200 μm. With launching into an undoped fiber, the pump coupling efficiency was measured to be approximately 80%. The pulse temporal behavior was recorded with a digital oscilloscope (LeCroy Wavepro 7100; 10G samples/sec; 1 GHz bandwidth) and a fast InGaAs photodiode. The laser spectrum was measured by an optical spectrum analyzer (OSA) with 0.1-nm resolution (Advantest Q8381A).
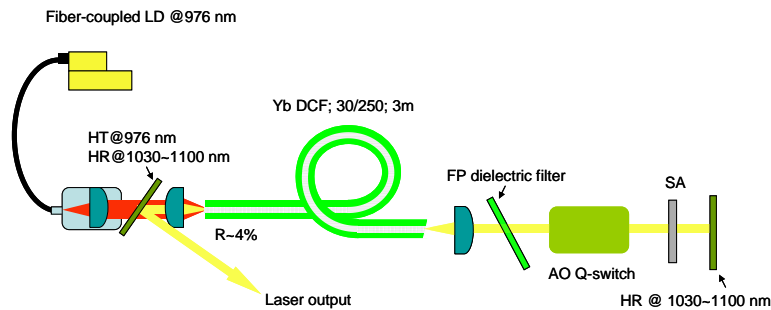

Fig. 1. Schematic diagram of the diode-pumped hybrid Q-switched Yb-doped double-clad fiber laser. HR, high reflection; HT, high transmission; SA, saturable absorber.

3. Results and discussions

Firstly the residual pump power were measured (single-pass) to be around 1.5%~2% of the launched pump power, meaning the absorption coefficient was nearly 6 dB/m. The value of absorption coefficient was lower than the specification and might be due to different spectral profile and beam quality of the pump source. The performances of the PQS fiber laser are shown in Fig. 2. Figure 2 (a) describes the dependence of average power on the pump power for continuous-wave (CW) and PQS operations. The threshold pump powers were both nearly 2 W for CW and PQS operation and the maximum average powers were 16 W and 14 W, respectively. The corresponding optical slope efficiencies were 74% and 67% for CW and PQS regimes, respectively. The roll-over at the highest pump power was attributed to the spectral shifting and broadening of the pump source. The Q-switching efficiency (the ratio of the maximum PQS power to the maximum CW power) was about 88%. The shortest pulse width was 60 ns obtained at a pump power of 24 W. Figure 2 (b) shows the dependences of pulse period and the ratio of timing jitter to pulse period on the launched pump power. As we increased launched pump power from 3 W to 24 W, the pulse period decreased from 512 μs to 31 μs and the ratio of timing jitter to pulse period was also found diminished from 12% to 2%. The oscilloscope traces of trains of the PQS laser at various pump power are shown in Fig. 2 (c).
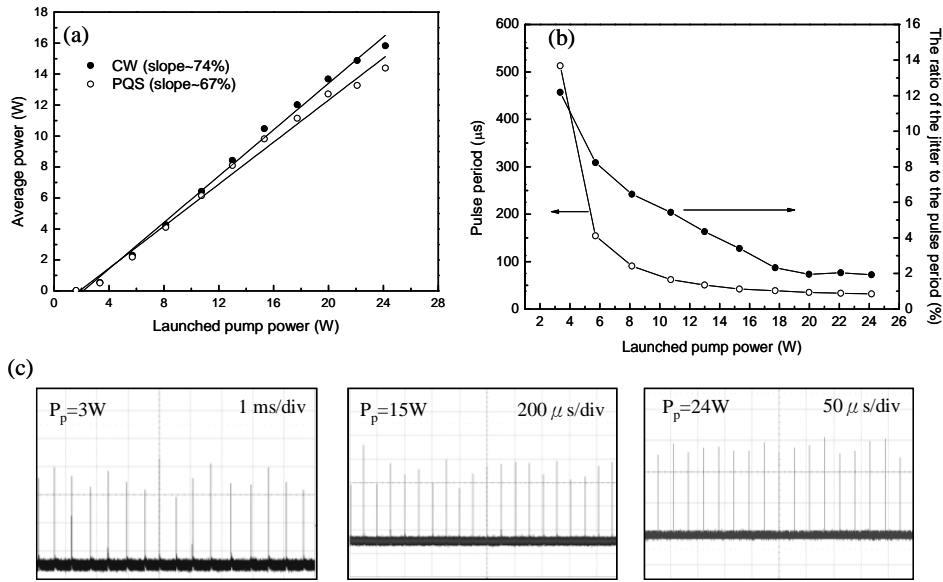
Fig. 2. (a) Dependence of average output power on the launched pump power for the CW and passive Q-switching operations; (b) dependence of pulse period and timing jitter on the launched pump power; (c) the oscilloscope traces of trains of the PQS pulses at various pump powers.

In order to improve the jitter, the AO Q-switch was inserted inside the external cavity. The diffraction efficiency of the AO Q-switch was measured to be about 30% by using the aforementioned CW fiber laser. The duty cycle of loss modulation of the AO Q-switch was set 90%, i.e. the ON-time of the RF-power was 90% of the pulse period. In the HQS operation, the pulse repetition rate of the HQS laser (f_{HQS}) could be operated stably between approximately 0.7 and 0.8 times the pulse repetition rate of the PQS laser (f_{PQS}) for all pump powers. In a conventional PQS laser, the pulse repetition rate is proportional to the cavity gain-to-loss ratio. Since AO Q-switch introduced additional losses in the cavity, the stable range of the f_{HQS} was less than the value of f_{PQS}. Figure 3 shows the oscilloscope traces of (a) the PQS pulses (period = 512μs) and (b) the HQS pulses (period = 620μs) at the pump power of 3W, respectively.
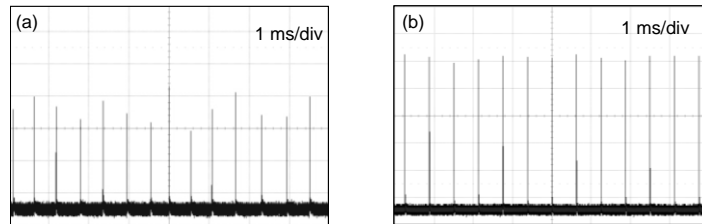

Fig. 3. The oscilloscope traces of trains of (a) the PQS pulses (period = 512μs) and (b) the HQS pulses (period = 620μs) at the pump power of 3W.

When the operational frequency in HQS configuration was out or range of stable region, the output pulse was found to be irregular. Figure 4 (a) shows the oscilloscope traces of trains of the HQS laser when f_{AO} was higher than $0.8 \times f_{PQS}$, where the output pulse train was extremely unstable. As the repetition rate of the AO Q-switch (f_{AO}) was decreased to lower than $0.7 \times f_{PQS}$, a prelasing effect occurred, as shown in Fig. 4 (b). The prelasing was attributed to the lasing by residual feedback within the low-Q time interval rather than

amplified spontaneous emission (ASE). Furthermore, we measured the lasing optical spectrum and confirmed no obvious ASE effect in HQS configuration.
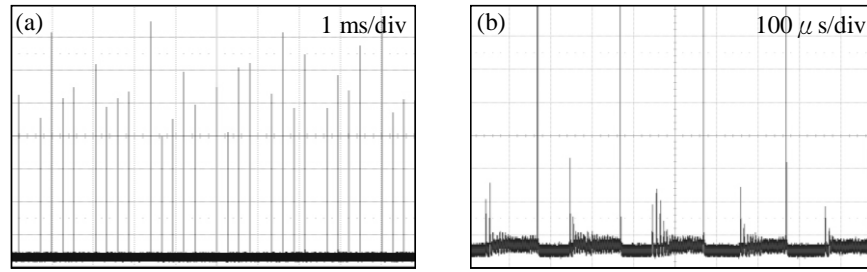

Fig. 4. The oscilloscope traces of trains of the HQS fiber laser when f_{AO} was (a) higher than 0.8 × f_{PQS} (b) lower than 0.7 × f_{PQS}.

To investigate the performances of the HQS laser, a pure AQS laser with the identical AO Q-switch was also demonstrated for comparsion. Figure 5 (a) and (b) presents the comparison of the pulse repetition rate and the pulse energy of the PQS laser, the HQS laser, and the AQS laser, respectively. The green and the blue regions represent the operational repetition rate and the pulse energy of the AQS laser and the HQS laser, respectively. As shown in Fig. 5 (a), at the pump power of 24 W the highest and the lowest pulse repetition rate of the pure AQS laser were 200 kHz and 54 kHz, respectively. Figure 5 (c) shows the oscilloscope of traces of trains of the pure AQS laser at various repetition rates under a pump power of 24W.
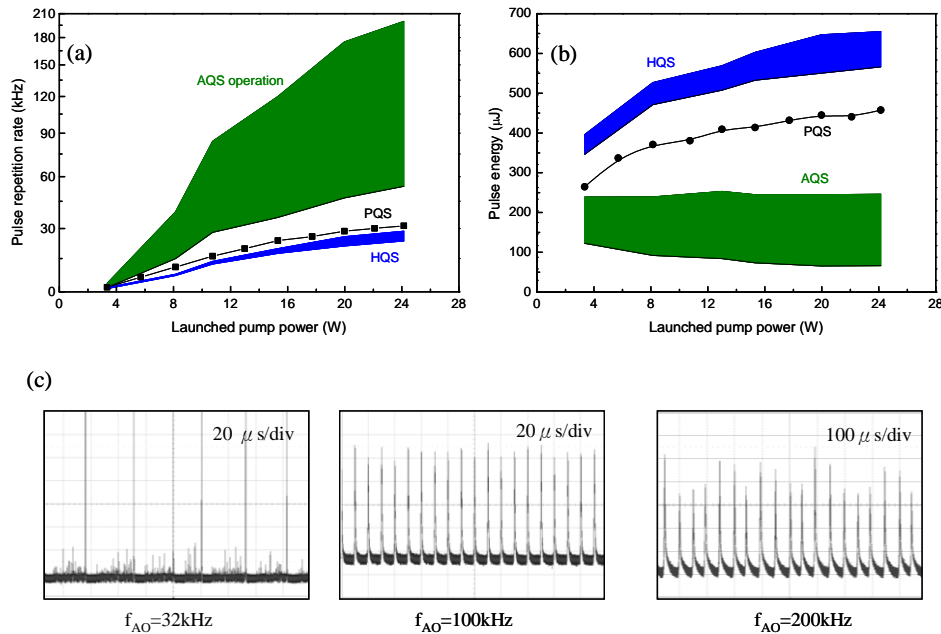

Fig. 5. (a) The pulse repetition rate of the pure PQS, the pure AQS, and the HQS lasers at the various launched pump powers ; (b) the pulse energy of the three lasers at the various launched pump powers. The green and the blue regions represent the operational repetition rate of the AQS laser and the HQS laser, respectively; (c) the oscilloscope traces of trains of pure AQS laser at various repetition rates under a pump power of 24 W.

The upper and the lower pulse repetition rates of the pure AQS laser were limited by low intracavity circulating photon density and the prelasing effect, respectively. On the other hand the pulse repetition rate of the HQS laser at the pump power of 24 W could be operated from

23.6 kHz to 28.6 kHz. In Fig. 5 (b), the maximum pulse energy of the HQS laser was 0.56 mJ, which was virtually twice higher than the pulse energy of the AQS laser and 25% higher than that of the PQS laser. The shortest pulse widths in the three regimes were 150 ns, 60 ns, and 50 ns for the AQS, the PQS, and the HQS lasers at the pump power of 24 W, respectively. Note that although the gain fiber could guide 15 modes (V number ~6), the M^2 beam-quality factors of the three regimes were measured to be <1.5 by coiling the fiber with a diameter of 10 cm.

For studying the jitter reduction, we measured the pulse period and the jitter of both the PQS and the HQS lasers at a pump power of 3 W where the PQS laser experienced the largest jitter. Figure 6 shows both the pulse period and the corresponding histogram for about 1000 pulses of the PQS and the HQS lasers, respectively. The average periods of the HQS and the PQS operations were 620 ± 0.074 μs and 512 ± 31 μs, respectively. The jitter is expressed in terms of the standard deviation of the pulse period. The jitter was reduced significantly from 62 μs to 140 ns which is almost the same as the jitter (~120 ns) obtained in the AQS fiber laser at the same pump power.
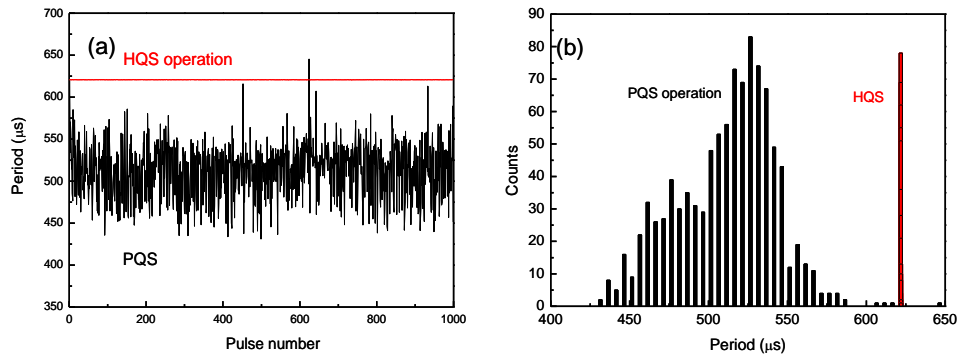

Fig. 6. (a) The pulse period and (b) the corresponding histogram of the pulse period of the PQS and the HQS lasers at the pump power of 3 W. The timing jitter is expressed in terms of standard deviation of the pulse period.

This result could be also observed in the previous experiments [12,13]. In Ref [12], the minimal jitter ~400 ns is slightly larger than the jitter of 200 ns obtained in their AQS laser. The larger jitter was attributed to the fact that the Cr^{4+}: YAG crystal absorber was not bleached fast enough when the AO Q-switch was opened (RF-power OFF). In contrast, the semiconductor absorber requires a shorter bleaching time due to the smaller saturation fluence of semiconductor absorbers compared to the Cr^{4+}:YAG crystal [4].

Moreover, to study the dependence of the jitter on the duty cycle of loss modulation, we varied the duty cycle from 0% (i.e. PQS operation) to 90% for three different pump powers of 3 W, 15 W, and 24 W. The f_{AO}^{-1} were set 620 μs for P_p of 3W, 55.56 μs for P_p of 15W, and 38.31μs for P_p of 24 W, respectively. Figure 7 depicts the dependence of the ratio of jitter to pulse period of the HQS laser on the duty cycle of loss modulation for the three pump powers. At the duty cycle = 0%, the jitters for the three pump powers were 62 μs (pump power, P_p = 3 W; period = 512 μs), 1.4 μs (P_p = 15 W; period = 54 μs), and 0.6 μs (P_p = 24 W; period = 38 μs). The ratios were reduced substantially at the duty cycle = 40%. At the pump power of 3W, the ratio was reduced greatly from 12% (jitter = 62 μs) to 0.05% (jitter = 0.3 μs). Besides, the ratios for the higher two pump powers decreased from 3.4% (jitter = 1.43 μs) to 0.35% (jitter = 0.2 μs) for P_p = 15 W and 1.9% (jitter = 0.61 μs) to 0.3% (jitter = 0.1 μs) for P_p = 24 W. Increasing continuously the duty cycle to 90%, the ratios decreased to 0.02% (140 ns) for P_p = 3W, 0.19% (100 ns) for P_p = 15 W, and 0.2% (80 ns) for P_p = 24 W. The minimal jitters were nearly the same results obtained in the AQS laser, implying that the restriction is mainly due

to the jitter of the pump scheme and the driving electronics of the AO Q-switch. The experimental result reveals that a further jitter-reduction would be achieved by using a more stable pump source and driving electronics.
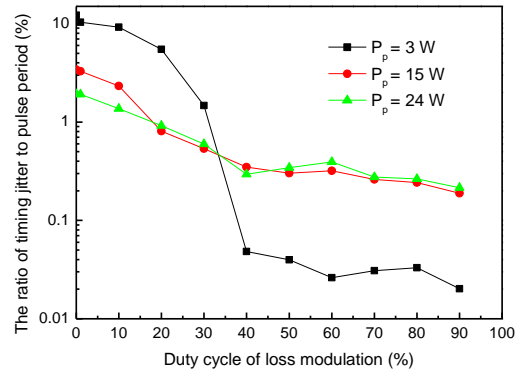

Fig. 7. The dependence of the ratio of jitter to pulse period of the HQS laser on the duty cycle of loss modulation for the pump power of 3W, 15W, and 24W. The f_{AO}^{-1} were set 620 μs for Pp of 3W, 55.56 μs for Pp of 15W, and 38.31μs for Pp of 24 W, respectively.

4. Conclusion

In conclusion, we have investigated the performance of a HQS fiber laser that was constructed with a low RF-power driven AO Q-switch and an AlGaInAs semiconductor saturable absorber. The HQS method combines the advantages of the passive Q-switching and the active Q-switching. Compared to a pure PQS fiber laser, the ratio of timing jitter to pulse period can be significantly reduced from 2% to 0.3% in the regime of far above threshold. On the other hand, the prelasing effect in a pure actively Q-switched fiber laser can be considerably improved. The maximum pulse energy of the HQS fiber laser can be increased approximately 100% and 25% in comparison with the results of the AQS and the PQS fiber laser, respectively. At a pump power of 24 W, the highest pulse energy is up to 0.56 mJ with the pulse duration of 50 ns at a repetition rate of 23 kHz.

Acknowledgments